Biomacromolecules

Subscriber access provided by Kaohsiung Medical University

Article

Surface Modification with a Catechol Bearing Polypeptide and Sensing Applications

Eda Aydindogan, Emine Guler Celik, Dilek Odaci Demirkol, Shuhei Yamada, Takeshi Endo, Suna Timur, and Yusuf Yagci

Biomacromolecules, **Just Accepted Manuscript** • DOI: 10.1021/acs.biomac.8b00650 • Publication Date (Web): 11 May 2018

Downloaded from http://pubs.acs.org on May 14, 2018

Just Accepted

"Just Accepted" manuscripts have been peer-reviewed and accepted for publication. They are posted online prior to technical editing, formatting for publication and author proofing. The American Chemical Society provides "Just Accepted" as a service to the research community to expedite the dissemination of scientific material as soon as possible after acceptance. "Just Accepted" manuscripts appear in full in PDF format accompanied by an HTML abstract. "Just Accepted" manuscripts have been fully peer reviewed, but should not be considered the official version of record. They are citable by the Digital Object Identifier (DOI®). "Just Accepted" is an optional service offered to authors. Therefore, the "Just Accepted" Web site may not include all articles that will be published in the journal. After a manuscript is technically edited and formatted, it will be removed from the "Just Accepted" Web site and published as an ASAP article. Note that technical editing may introduce minor changes to the manuscript text and/or graphics which could affect content, and all legal disclaimers and ethical guidelines that apply to the journal pertain. ACS cannot be held responsible for errors or consequences arising from the use of information contained in these "Just Accepted" manuscripts.

ACS Publications

is published by the American Chemical Society. 1155 Sixteenth Street N.W., Washington, DC 20036

Published by American Chemical Society. Copyright © American Chemical Society. However, no copyright claim is made to original U.S. Government works, or works produced by employees of any Commonwealth realm Crown government in the course of their duties.

Surface Modification with a Catechol Bearing Polypeptide and Sensing Applications

Eda Aydindogan[†], *Emine Guler Celik*[†], *Dilek Odaci Demirkol*[†], *Shuhei Yamada*[§], *Takeshi Endo*[§], *Suna Timur*[†⊥*], *Yusuf Yagci*[‡#*]

[†]Department of Biochemistry, Faculty of Science, Ege University, 35100, Bornova, Izmir, Turkey

[§]Molecular Engineering Institute, Kinki University, 11-6 Kayanomori, Iizuka, Fukuoka 820-8555, Japan

[⊥]Central Research Testing and Analysis Laboratory Research and Application Center, Ege University, 35100, Bornova, Izmir, Turkey

[‡]Department of Chemistry, Faculty of Science and Letters, Istanbul Technical University, 34469, Maslak, Istanbul, Turkey

[#]King Abdulaziz University, Faculty of Science, Chemistry Department, Jeddah/Saudi Arabia

ABSTRACT

A novel catechol bearing polypeptide (CtP) was synthesized and used as a component of electrochemical biosensor involving both enzymatic activity and affinity-based sensing systems. Glucose oxidase (GOx) and Anti-Immunoglobulin G (Anti-IgG) were selected as model biorecognition elements for the selective analysis of glucose and IgG. Step by step surface modifications were followed using various techniques such as cyclic voltammetry (CV) and electrochemical impedance spectrometry (EIS) as well as X-Ray photoelectron spectroscopy (XPS). Additionally, contact angles were measured in order to observe surface properties. Amperometric measurements using GOx biosensor, were performed at -0.7 V by following the oxygen consumption due to the enzymatic reaction in different glucose concentrations. Affinity based interactions via IgG sensor was monitored using differential pulse voltammetry (DPV) technique. As the 'surface design with CtP' approach employed herein is generally applicable and easily adaptable to obtain functional matrices for biomolecule immobilization, CtP coated surfaces can be promising platforms for the fabrication of various bio-based sensing systems.

KEYWORDS

Catechol, Polypeptide, Functional Polymers, Protein immobilization, Biosensor

INTRODUCTION

Polymers bearing functional structures such as polypeptides and poly(ethylene glycol) chains etc. have received great interest as they can be used in biomedicine, drug delivery, nanoscale self-assembly or tissue engineering. Their specific characteristics are associated with the recognition properties like antibody-antigen interactions, biodegradability, catalytic activity mimicking and biocompatibility.[1-5] Polypeptides, prepared by using primary and tertiary amine initiators,[6,7] can form α-helix, β-sheet and random coil structures, and self-assembly. As they possess these unique characteristics, they give different properties to any polymeric material they are attached.[8,9]

Affinity-based sensing systems using different methods such as fluorescence-based[10-12] and colorimetric immunoassays,[13,14] paper-based lateral flow immunoassays[15,16] and electrochemical biosensors[17,18] are being used in various fields as sensing systems. Electrochemical biosensors have gained interest in detecting different biomolecules as they give fast response with high sensitivity and can be worked with small amounts of samples easily. Recent literature clearly verifies the popularity of electrochemical biosensors; as different analytes including glycoproteins,[19,20] hydrogen peroxide,[21] proteins,[22,23] glucose,[24-28] mycotoxins[29] and nucleic acids,[30-34] with different recognition agents such as aptamers, proteins, enzymes and red blood cell membranes as well as electroactive labels (nanoparticles, quantum dots etc.) were successfully used. The biomimetic properties of artificial interfaces mimicking different biological and environmental systems are being used in electrochemical biosensing systems to investigate biological processes.[35-37] Recent developments in this promising field have been covered by several review articles.[38-42]

Herein, we report the use of catechol bearing polypeptide (CtP) as an electrochemical sensing platform. Recently, polypeptide bearing monomers have been synthesized and successfully polymerized onto various electroactive substrates serving as both immobilization and sensing/bio-recognition surfaces.[43-46] This work has been conducted starting with the synthesis of the catechol-functional polypeptide and the surface modification of an electroactive surface (glassy carbon electrode; GCE) with this novel polymeric structure. Catechol has been widely used as an anchoring molecule to attach functional molecules and polymers to the surface of nanoparticles, metal oxide materials, electrodes etc. Synthetic strategies for the preparation of catechol functional polymers have been extensively investigated. [47-49]

In the present work, protected dopamine was used as an initiator for the ring opening polymerization. The *N*-carboxy anhydride ring formation and simultaneous ROP followed by deprotection processes facilitated synthesis of catechol functional polypeptide with well-defined structures. As model biomolecules, glucose oxidase (GOx) and Anti-Immunoglobulin G (IgG) were selected to investigate the potential use of this polymeric architecture as two different biosensor systems, namely enzymatic activity and affinity interactions, respectively. These biofunctional surfaces were used as working electrodes through the electrochemical measurements. Surface modifications were registered by cyclic voltammetry (CV) and electrochemical impedance spectrometry (EIS) as well as X-Ray photoelectron spectroscopy (XPS). Contact angles of the surfaces after coating and biomolecule binding were also measured. Also, interfering compounds were applied to the modified surfaces to monitor the selectivity and specificity of the proposed sensing system. Response signals of GOx biosensor were monitored using amperometric measurements at -0.7 V by following the oxygen consumption stemming from the glucose oxidation by the GOx. In the case of affinity-based sensor, the sensing

performance was proved using differential pulse voltammetry (DPV) data with different concentrations of IgG in the presence of a water soluble redox probe and a calibration curve obtained using the decrease in the signal responses as a result of selective capturing of IgG by Anti-IgG immobilized surface.

EXPERIMENTAL SECTION

Reagents. Hydrogen bromide (30% in acetic acid, ca. 5.1 mol/L), acetic acid, triethylamine, 3,4-dihydroxybenzonitrile, phosphorus pentoxide, Lithium aluminum hydride were purchased from Tokyo Chemical Industry used as received. All other solvents used in polymer synthesis were purchased from Wako Pure Chemical Industries, Ltd. Glutaraldehyde solution (Grade II, 25%), Glucose oxidase (Type X-S, lyophilized powder), Glucose (Bio-Xtra, ≥99.5%), Anti-Bovine IgG antibody (whole antiserum), IgG from bovine serum (reagent grade, ≥95%), Uric Acid (UA) (≥99%, crystalline), Ascorbic Acid (AA) (BioXtra, ≥99.0%, crystalline), Bovine Serum Albumin (BSA) (lyophilized powder, ≥96% (agarose gel electrophoresis)) and potassium hexacyanoferrate (III) (HCF) was obtained from Sigma (St. Louis, MO, USA).

Apparatus. For polymer synthesis and characterization; NMR (400 MHz) spectra were recorded with a JEOL ECS-400 spectrometer, and the chemical shifts were given in ppm using tetramethylsilane (TMS) as an internal standard. Fourier transform infrared spectroscopy (FT-IR) analysis was carried out on a Thermo Scientific Nicolet iS10 in the 600–4000 cm^{-1} ranges. Size exclusion chromatography (SEC) was carried out on a TOSOH HLC-8220 system equipped with three consecutive polystyrene gel columns [TSK- gels (bead size, exclusion limited molecular weight); super- AW4000 (6 μm, > $4x10^5$), super-AW3000 (4 μm, > $6x10^4$), and super-AW2500

(4 μm, > $2x10^3$)] and refractive index and ultraviolet detectors at 40°C. The system was operated using 10 mM LiBr in *N*,*N*-dimethylformamide (DMF) as the eluent at a flow rate of 0.5 mL min^{-1}. Polystyrene standards were employed for calibration.

PalmSens Potentiostat (Palm Instruments, Houten, Netherlands) was used for the electrochemical analyses which are differential pulse voltammetry (DPV) and cyclic voltammetry (CV) for this study. Amperometric measurements were performed in 10 mL sodium acetate buffer (50 mM, pH 4.5) under ambient conditions at -0.7 V potential to monitor the enzymatic activity on the electrode surface. Electrochemical impedance spectroscopy (EIS) was also used for characterization of the GCE surface which was implemented with a CHI 6005 C model electrochemical analyzer (CH Instruments Incorporation, Austin, Texas, USA). A three-electrode system was established with a glassy carbon electrode (GCE) as a working electrode, a platinum (Pt) electrode as a counter electrode and Ag/AgCl (3.0 M KCl, Metrohm, Switzerland) electrode as a reference electrode. To analyze the modification of GCE, CV and EIS techniques (frequency range from 0.03 Hz to 10 kHz at +0.18 V) were used as characterization techniques for the surfaces designed on GCE by using HCF. Using the sessile drop method with a CAM100 KSV (KSV, Finland), contact angle measurements were performed with a drop of Milli-Q water (4.0 μL). Changes in contact angle were monitored using a CCD camera. The surface modifications as a result of biomolecule binding were confirmed via X-ray photoelectron spectrometer (Thermo Scientific, USA). XPS analyses were performed on a mono-chromated Al Kα radioactive source. All experiments were conducted at ambient conditions.

Synthesis. Synthetic pathways for all intermediates and their molecular structures are presented in Schemes 1-3.

Synthesis of N-phenoxycarbonyl-L-Lysine with oligoethylene oxide

The *N*α-phenoxycarbonyl derivative of *N*ε-(carbobenzyloxy)-L-Lysine **1**, was prepared according to the literature.[50] To the mixture of **1** (6.0 g, 15.0 mmol) and acetic acid (2.5 mL), hydrogen bromide (30% in acetic acid, ca. 5.1 mol/L) (10.0 mL, 51.0 mmol) was slowly added at 0°C to remove the *N*ε-carbobenzyloxy group. After stirring for 1 h at room temperature, diethyl ether (100 mL) and distilled water (50 mL) was added into the reaction mixture. The aqueous phase was separated and concentrated to give a desired compound **2** as a viscous liquid (Scheme 1). ^{1}H NMR (400 MHz, DMSO-d_6, δ, ppm): 1.25-1.85 (m, 6H), 2.70-2.85 (m, 2H), 3.91-4.00 (m, ^{1}H), 7.07 (d, 2H, J = 7.8 Hz), 7.19 (t, 1H, J = 7.3 Hz), 7.36 (t, 2H, J = 7.8 Hz), 7.76 (br, 3H), 8.07 (d, 1H, J = 7.8 Hz). ^{13}C NMR (100 MHz, DMSO-d_6, δ, ppm): 22.60, 26.49, 30.15, 38.59, 53.85, 121.60, 125.05, 129.33, 150.94, 154.48, 173.49.

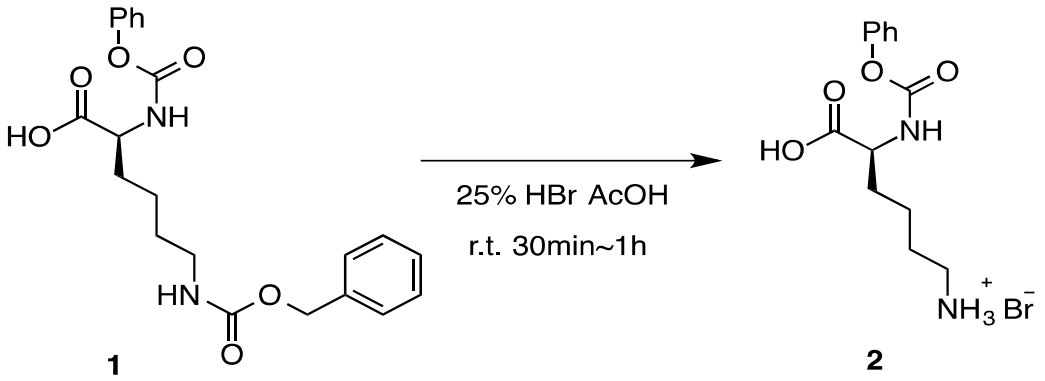

Scheme 1. Removal of *N*ε-carbobenzyloxy group from *N*ε-(carbobenzyloxy)-L-Lysine.

Activated ester-containing oligoethylene oxide **3** prepared according to the literature[51] and used for the conjugation of oligoethylene oxide moiety into the side chain of activated urethane derivative (Scheme 2).

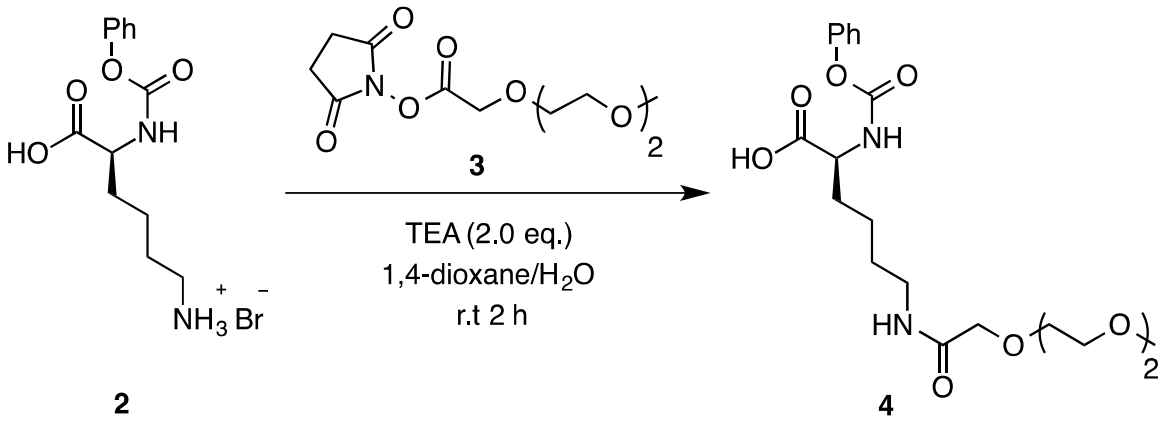

Scheme 2. Conjugation of oligoethyleneoxide into N-phenoxycarbonyl-L-Lysine.

Experimentally, to a solution of **2** (4.2 g, 12 mmol) in 1,4-dioxane (15 mL) and water (5.0 mL), **3** (3.9 g, 14 mmol) was added dropwise. Triethylamine (2.4 g, 24 mmol) was added at 0 °C and continued to stir for 2 h at room temperature. The resulting mixture was poured into distilled water (100 mL), and then extracted with ethyl acetate (3×100 mL). The combined organic layer was dried over Na_2SO_4, filtered, and concentrated under reduced pressure. The crude products were purified by column chromatography (elution with the mixture of dichloromethane/methanol, 93:7 vol.%) to give 4.3 g (10.2 mmol, 85 %) of the compound **4** as a viscous colorless oil which solidified slowly on standing; m_p = 57.1–58.7 °C. ^{1}H NMR (400 MHz, DMSO-d_6, δ, ppm): 1.26-1.53 (m, 4H), 1.57-1.84 (m, 2H), 3.02-3.16 (m, 2H), 3.24 (s, 3H), 3.40-3.50 (m, 2H), 3.52-3.62 (m, 6H), 3.85 (s, 2H), 3.90-4.02 (m, 1H), 7.08 (d, 2H, J = 8.12 Hz), 7.19 (t, 1H, J = 7.38 Hz), 7.37 (t, 2H, J = 7.82 Hz), 7.68 (br, 1H), 8.05 (d, 1H, J = 7.88 Hz). ^{13}C NMR (100 MHz, DMSO-d_6, δ, ppm): 23.57, 29.35, 30.97, 38.41, 54.53, 58.61, 70.05, 70.14, 70.49, 70.83, 71.82, 122.13, 125.50, 129.81, 151.57, 154.97, 169.59, 174.15. IR (neat, cm^{-1}): 3300, 2872, 1738, 1614, 1200, 1093.

Synthesis of acetonide-protected 3,4-dihydroxybenzylamine

The protected amino functional initiator was prepared according to Scheme 3.

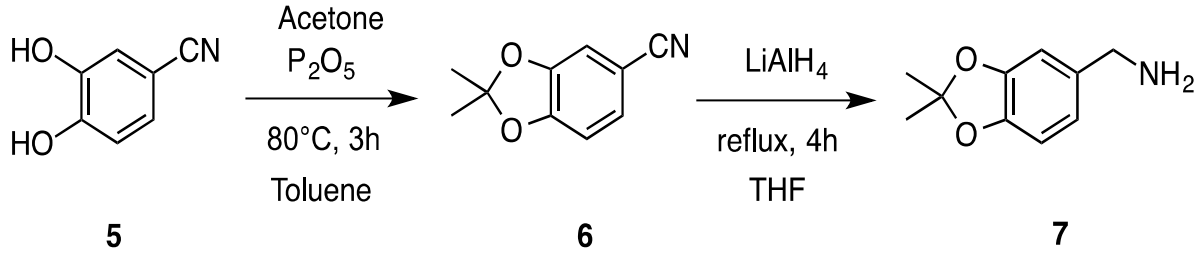

5 **6** **7**

Scheme 3. Synthesis of acetonide-protected 3,4-dihydroxybenzylamine.

To a suspension of 3,4-dihydroxybenzonitrile **5** (2.7 g, 20 mmol) and phosphorus pentoxide (4.2 g, 30 mmol) in toluene (40 mL), acetone (2.3 g, 40 mmol) was added and stirred at 80°C for 3 h. After cooling to room temperature, 2.0 N NaOH aqueous solution was added to adjust pH to be neutral and then extracted with ethyl acetate. The combined organic layer was dried over Na_2SO_4, filtered, and concentrated under reduced pressure. The crude product was purified by column chromatography (elution with the mixture of ethyl acetate/hexane, 1:7 vol.%) to give a catechol-protected compound **6** (25%). ^{1}H NMR (400 MHz, chloroform-*d*, δ, ppm): 1.70 (s, 6H), 6.76 (d, 1H, J = 7.96 Hz), 6.93 (d, 1H, J = 1.72 Hz), 7.16 (dd, 1H, J = 8.24, 1.80 Hz). ^{13}C NMR (100 MHz, chloroform-*d*, δ, ppm): 25.99, 104.31, 109.03, 111.30, 119.30, 120.22, 127.80, 147.86, 151.40. Lithium aluminum hydride (370 mg, 9.7 mmol) was added to a solution of the obtained compound **6** (850 mg, 4.8 mmol) in tetrahydrofuran (20 mL) and the mixture was refluxed for 4 h. After cooling to room temperature, 2.0 N NaOH aqueous solution (1.0 mL) was added to the resulting mixture. The mixture was filtered through a pad of celite, and the filtrate was concentrated under reduced pressure to give 644 mg (7.3 mmol, 75%) of target compound **7** as colorless oil. ^{1}H NMR (400 MHz, chloroform-*d*, δ, ppm): 1.47 (s, 2H), 1.66 (s, 6H), 3.74 (s, 2H), 6.60-6.72 (m, 3H). ^{13}C NMR (100 MHz, chloroform-*d*, δ, ppm): 25.95, 46.57, 107.69, 108.08, 117.81, 119.57, 136.93, 146.34, 147.76.

Preparation of CtP by chain growth polycondensation of N-phenoxycarbonyl-L-lysine derivative

The urethane derivative **4** (426 mg, 1.0 mmol) and acetonide-protected 3,4-dihydroxybenzylamine 7 (5.56 mg, 0.04 mmol) were dissolved in anhydrous DMAc (2.0 mL) (initial feed ratio, [4]:[7] = 25:1), and the mixture was added to a Schlenk tube. The resulting mixture was stirred at 60°C for 12 h under a nitrogen atmosphere. The reaction mixture was cooled to room temperature and poured into diethyl ether (150 mL). The resultant precipitate was collected and then dried under vacuum to give 0.24 g (81%) of target polypeptide as a sticky powder, (M_n = 5,700, M_w/M_n = 1.43, estimated by SEC analysis). Deprotection of acetonide group was conducted by acid treatment of obtained polypeptide. The polypeptide (200 mg) was dissolved in the methanol (5.0 mL) and water (1.0 mL), and then 4.0 N HCl/1,4-dioxane (2.0 mL) was added slowly. The mixture was stirred at room temperature for 12 h. The resulting mixture was poured into diethyl ether (150 mL) and formed precipitate was collected and then dried under vacuum to give 184 mg (92%) of CtP. ^{1}H NMR (400 MHz, DMSO-d_6, δ, ppm): 1.20-2.11 (br, 6H), 3.01-3.22 (br, 2H), 3.26-3.60 (br, 11H), 3.71-4.12 (br, 3H). IR (neat, cm^{-1}): 3291, 2872, 1648, 1537, 1093.

Surface modification of the GCE, electrochemical characterization and measurements. Initially, GCE was polished with 0.1 micron alumina slurry to get a mirror-like surface and bath sonicated for 5 min. in ethanol: distilled water (1:1) solution and then with only distilled water. Biosensor surface for the GOx-based biosensor was constructed as follows: GOx was immobilized on polymer covered electrode surface using GA as a cross-linker and the response signals related with the enzymatic reaction was measured by the injection of different concentrations of glucose solutions. Briefly, 5.0 μL polymer solution (0.5 mg/mL stock solution

in dimethyl formamide (DMF)) was drop casted on GCE surface and dried at ambient conditions to form a thin layer on the surface. The optimum polymer concentration was determined according to the signal response. Afterwards, GOx (1.0 mg in 5.0 μL 50 mM sodium phosphate buffer, pH 7.4) was mixed with 5.0 μL of GA (1.0% v/v in 50 mM sodium phosphate buffer, pH 7.4) and dropped on the surface, then, allowed to react at room temperature, to form a biolayer together with the polymer on GCE. Following the immobilization of the enzyme, biosensor responses were monitored with chronoamperometry at -0.7 V. In the measurement procedure, the biosensor was initially incubated in the sodium acetate buffer (50 mM, pH 4.5) for 5 min to activate the enzyme and different amounts of glucose from 0.1 M stock solution were added to 10 mL working buffer solution. This pH value was chosen as the best working condition, according to the literature. [52] After a baseline was observed, glucose was added and changes in the response signals were observed for another 200 s. Glucose solutions (0.01 – 5.0 mM) were prepared in working buffer, each measurement were taken in triplets and a calibration curve was obtained depending on the amperometric signals vs substrate concentrations. Surface characterization was done with CV (potential range, from -0.4 to +0.8 V), and EIS measurements. Biosensor surface was rinsed with Milli-Q water after each step, before and after the measurements to avoid unbound species.

For the affinity-based biosensor, first, GCE surface was covered with 5.0 μL CtP (0.5 mg/mL stock solution in dimethyl formamide (DMF)) as already described for the previous biosensor. Following, 20 μL anti-IgG antibody (100 μg/mL in sodium phosphate buffer, pH 7.4) was immobilized on the polymeric surface using GA as the same procedure with the GOx biosensor. To obtain sensor responses DPV signals were followed using the redox mediator (HCF, 5.0 mM), prior and after capturing of IgG by the anti-IgG immobilized surface. The drop-in response

signals were obtained as a result of selective interaction of Anti-IgG and IgG that prevents electron transfer efficiency towards the electroactive GCE surface. To obtain a calibration graph (between the difference in the current signals and concentration), different concentrations of 10 μL IgG (0.05 – 10 ng/mL in sodium phosphate buffer, pH 7.4) was dropped on the surface. CV and EIS techniques were also used to prove, surface covering, antibody immobilization and selective recognition of IgG. For contact angle and XPS measurements, all surface modifications were done with the same concentrations and amounts used for the analytical experiments, except they were done on an ITO glasses for CtP, CtP-GOx and CtP-Anti-IgG surfaces, separately.

To control the specificity and selectivity, control experiments with interfering compounds were conducted. For enzymatic activity-based biosensor with GOx, UA, AA and BSA was added to the working probe and signal responses were recorded with enzyme-modified GCE and compared with the glucose at the same concentration (0.1 mM). Similarly, for the affinity-based sensing system, selected interfering compounds, which are AA and BSA, were drop-casted on the Anti-IgG coated GCE and current signal response changes were compared with the IgG at the same concentration (1.0 ng/mL).

RESULTS AND DISCUSSION

Based on the methodology for the synthesis of polypeptide by chain growth polycondensation of N-phenoxycarbonyl derivative of α-amino acid, preparation of CtP was conducted (Scheme 4). In this study, poly(-L-Lysine) attached with oligoethylene oxide on side chain was designed in order to provide high solubility in aqueous media. Acetonide-protected catechol amine was used as an initiator for polycondensation of N-phenoxycarbonyl derivative. Chain-growth

polycondensation proceed smoothly at 60 °C to give a corresponding polypeptide. The obtained polypeptide shows high solubility for common organic solvents such as methanol, DMF, acetone, chloroform, and water. The molecular weight and polydispersity index were determined by SEC analysis to be 5700 g mol^{-1} and 1.43, respectively. Acetonide-protected catechol moiety at the terminal group was evidenced by the presence of proton signals in the ^{1}H NMR spectrum at 6.8 ppm (Figure 1). The acetonide group was successfully removed by hydrolysis using hydrogen chloride.

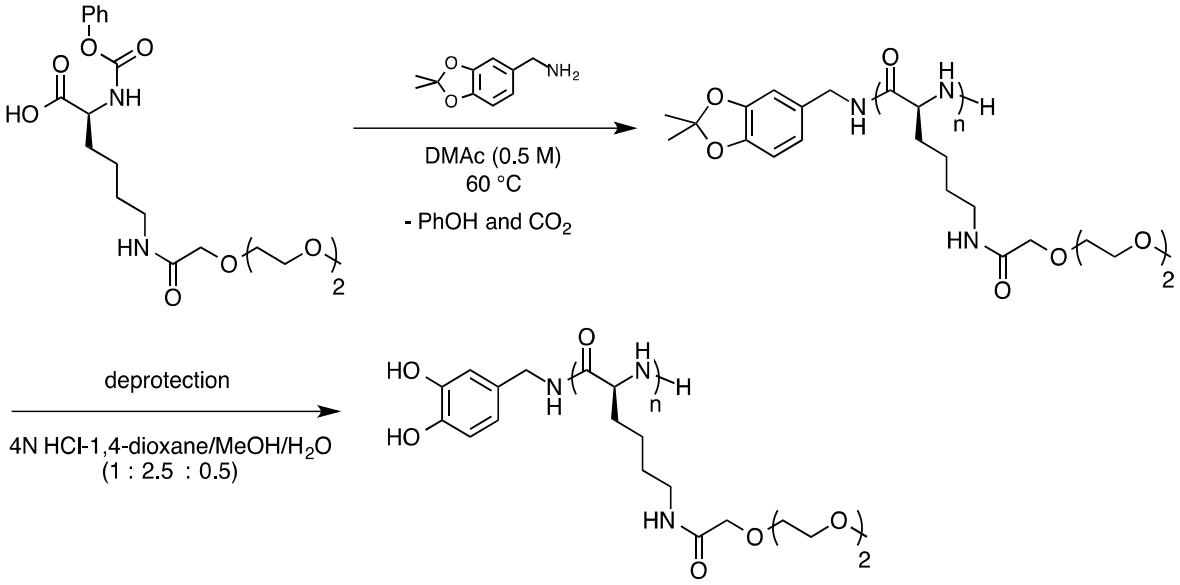

Scheme 4. Synthesis of catechol-attached polypeptide (CtP).

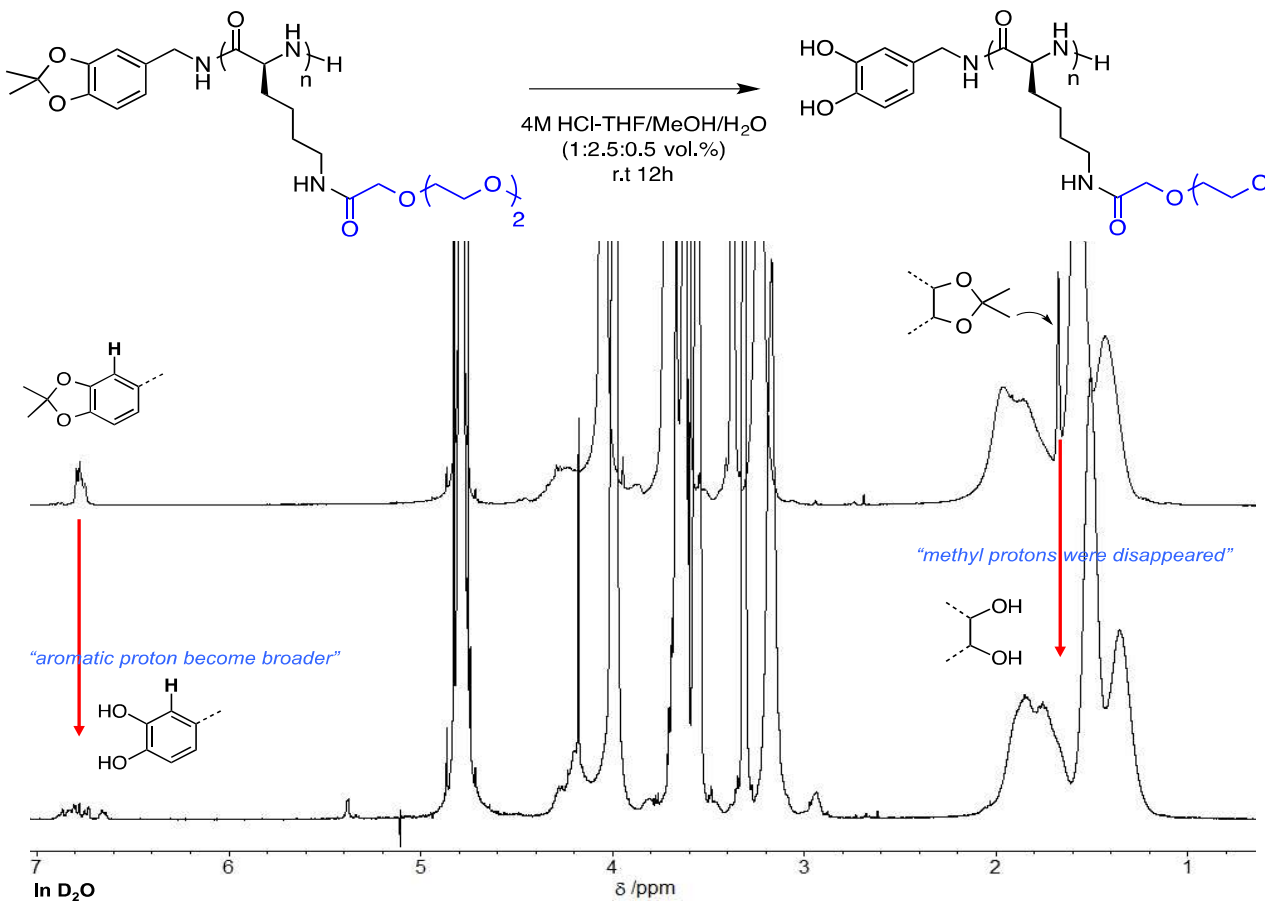

Figure 1. ^{1}H NMR spectra of acetonide- and catechol-bearing polypeptide.

Surface characterization and analytical features of GOx biosensor. Response signal of GOx biosensor was monitored by creating a modified GCE surface starting with the functionalization with CtP, followed by the immobilization of the enzyme to the surface by using glutaraldehyde (GA) as a cross-linker. Schematic representation of the surface modification and principles of electrochemical measurement of current signals are shown in Scheme 5.

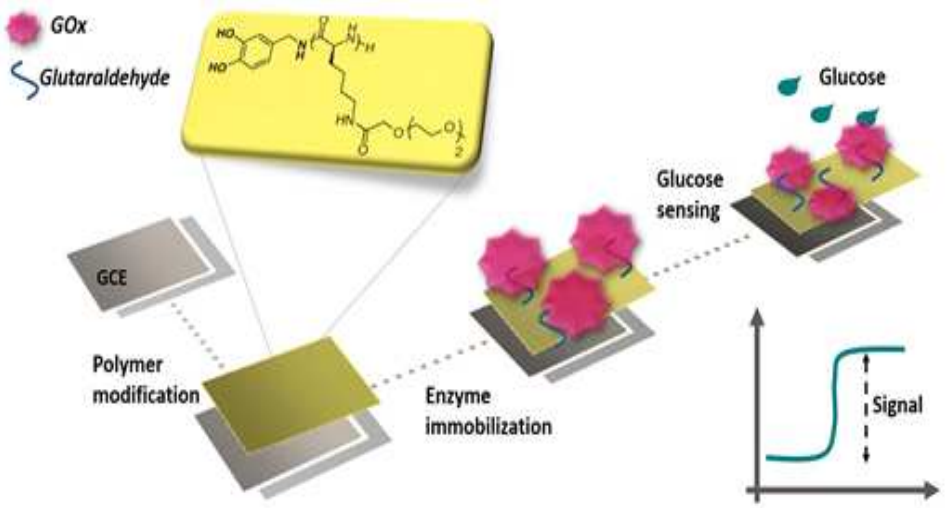

Scheme 5. Schematic representation of the preparation of GOx biosensor.

CV and EIS measurements which were taken stepwise for each surface modification, are given in Figure 2 (A and B). As can be seen from Figure 2A, modifications through polymer coating and biomolecule binding formed bulkier structures on the surface that prevent possible electron transfer processes occurring as the redox reaction takes place in the probe. Consequently, anodic and cathodic peaks were significantly decreased, confirming the successful modification on the GCE surface. Bare The measured anodic current peaks were found to be for Bare GCE: 42.697 μA (peak-to-peak separation of 0.084 V), for GCE-CtP: 18.396 μA (peak-to-peak separation of 0.434 V), and for GCE-CtP/GOx: 7.613 μA (peak-to-peak separation of 0.520 V). Similarly, cathodic current peaks were obtained as follows: Bare GCE 41.909 μA, GCE-CtP 22.839 μA, GCE-CtP/GOx 11.67 μA.

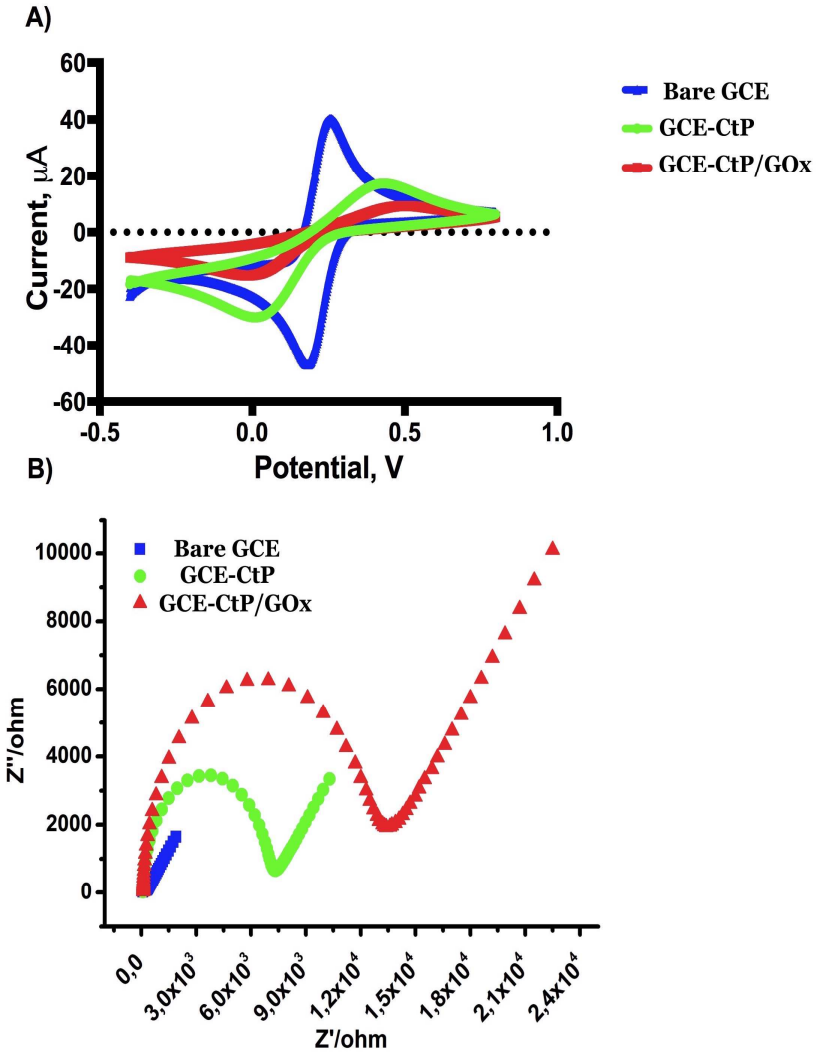

Figure 2. A) CV of Bare GCE, GCE-CtP, GCE-CtP/GOx surfaces. B) Nyquist diagrams of Bare GCE, GCE-CtP, GCE-CtP/GOx surfaces. [Randle's equivalent circuit was used to fit Nyquist plots and fitted graphs were given]. [All experiments were carried out in 50 mM sodium phosphate buffer (pH 7.4) containing 5.0 mM $[Fe(CN)_6]^{3-/4-}$ and 0.1 M KCl].

Furthermore, EIS also proves the successful modification of the GCE surface by showing the increase on the resistance in accordance with the step-by-step modification. EIS data were analyzed using the circuit design which includes solution resistance (Rs), Warburg impedance

(Zw) resulting from the diffusion of redox probe, the double layer capacitance (Cdl) and the change of the electron transfer resistance (Rct). As seen in the Figure 2B, a considerable increase was observed on the resistance after the surface modification with the CtP. The increase in the resistance values was even more pronounced for the surface after GOx immobilization. Rct values of Nyquist plots calculated for the designed biosensor at various stages were; Bare GCE: 161.1 Ω, GCE-CtP: 6837 Ω, and GCE-CtP/GOx: 12280 Ω.

Initially, signal responses of GOx biosensor were investigated. GOx worked as an electron flow monitoring agent on the surface, tracking the oxygen consumption rate. Based on the oxidation reaction of β-D-glucose to glucono-D-lactone, GOx was reduced. Consuming the molecular oxygen in the working buffer, it was oxidized to its original state, releasing hydrogen peroxide as a side product. The measured current signal was increased correlated with the increasing concentration of the glucose added to the working buffer solution. A calibration curve, given in Figure 3, was obtained using the correlated increase on the current signals (ΔI). After addition of glucose to working buffer, a rapid increase in the current signal indicates the enzymatic activity on the surface. The linear range was obtained in between 0.01-1.0 mM glucose, which corresponds to 1.8-180 μg/mL. The equation for the linear plot in the interval was calculated as $y = 3.321x - 0.1869$ and the R^2 was 0.9868.

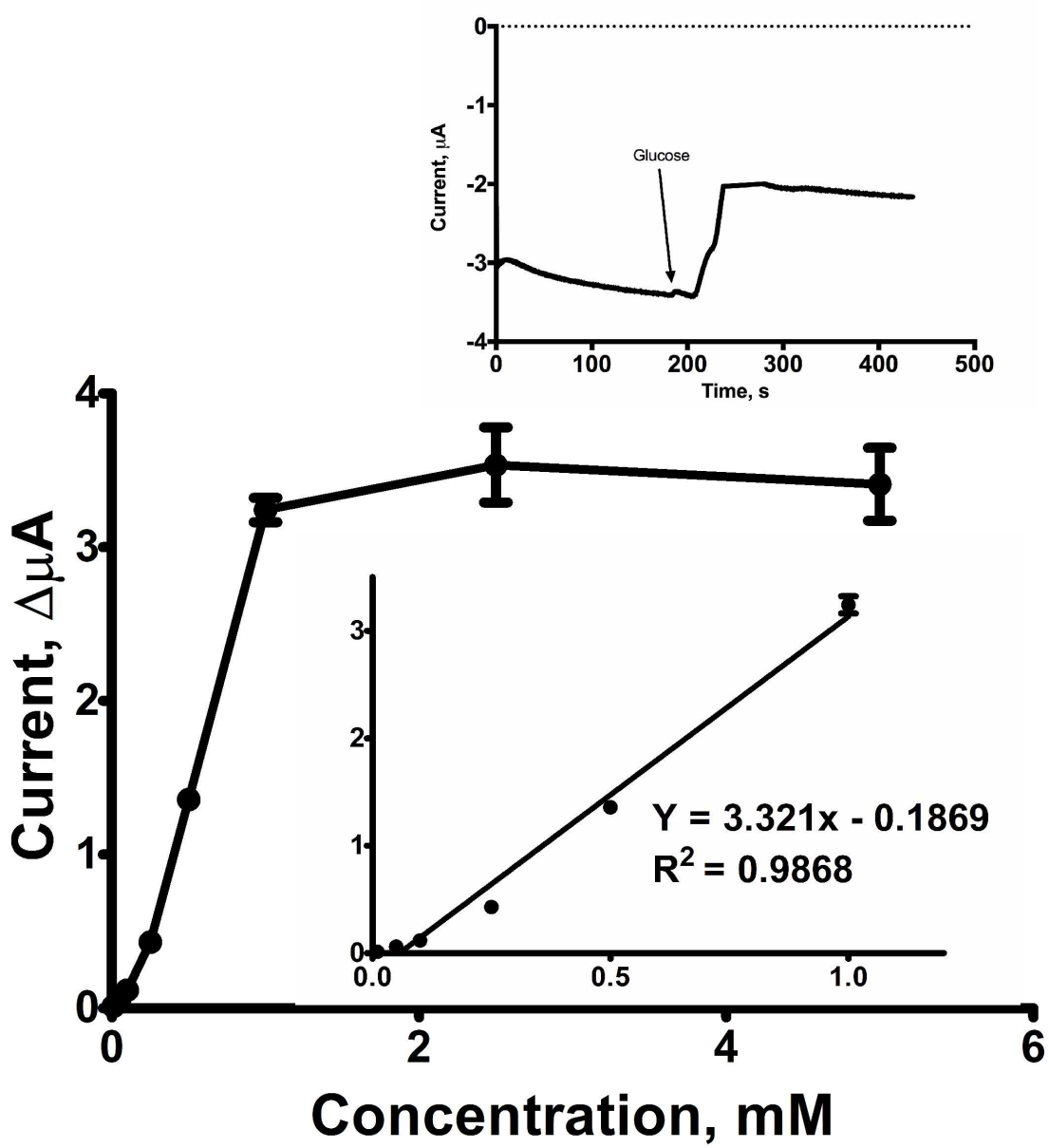

Figure 3. The calibration curve of GCE-CtP/GOx in response to different concentration of Glu solutions obtained by amperometric measurements (In 50 mM sodium acetate buffer, pH 4.5, 25°C, −0. 7 V. Error bars show ± S.D.).

Surface characterization and analytical features of affinity-based IgG Sensor. Initially similar strategy applied for the GOx immobilization was followed. Basically, Anti-IgG antibody

was bound to CtP with GA and different concentrations of IgG was then applied on the surface to facilitate observation of antibody/antigen interactions. Schematic representation for the surface modification and the basis of sensing responses were given in Scheme 6.

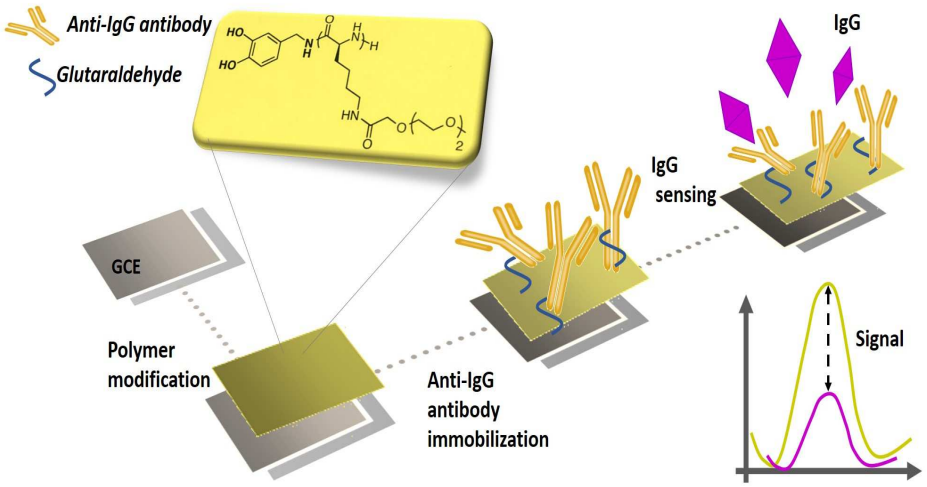

Scheme 6. Schematic representation of the preparation of affinity-based biosensor.

Modifications at each stage were followed using CV and EIS techniques and obtained data were given in Figure 4.

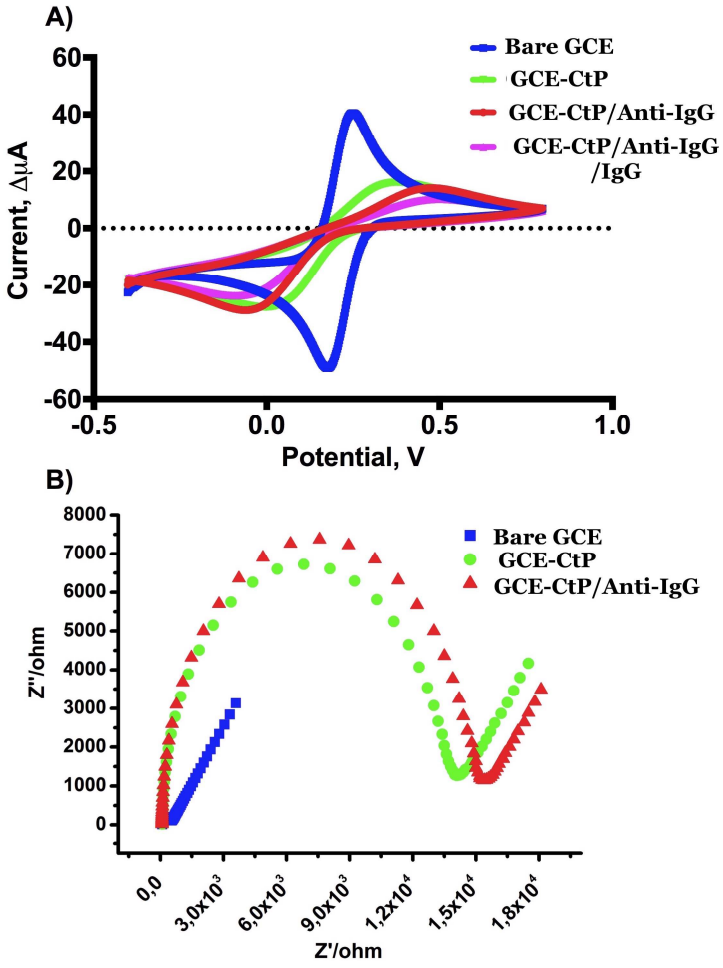

Figure 4. A) CV of Bare GCE, GCE-CtP, GCE-CtP/Anti-IgG and GCE-CtP/Anti-IgG/IgG surfaces. B) Bare GCE, GCE-CtP, GCE-CtP/Anti-IgG and GCE-CtP/Anti-IgG/IgG surfaces. [Randle's equivalent circuit was used to fit Nyquist plots and fitted graphs were given]. [All experiments were carried out in 50 mM sodium phosphate buffer (pH 7.4) containing 5.0 mM $[Fe(CN)6]^{3-/4-}$ and 0.1 M KCl].

Figure 4A clearly shows the successful modification of the surface as the current gets lower in each step of the procedure in the presence of the mediator. The observed reduction in the current power is due to the preclusion of electron transfer reactions. GCE measures the potential of the redox probe, $Fe(CN)_6^{4-}$ being oxidized to $Fe(CN)_6^{3-}$ and $Fe(CN)_6^{3-}$ being reduced to $Fe(CN)_6^{4-}$ in

the forward and backward measurements, respectively. GCE acts as both oxidant and reductant surfaces in the reversible process. The application of higher amount coating material would effect the current flow through the electrode surface. Consequently, the redox reaction stated above would become more difficult to monitor with increasing concentrations on the surface, and essentially resulting in a decrease in the current signal peaks. Anodic current peaks were measured as follows: Bare GCE 45.898 μA (peak-to-peak separation of 0.074 V), GCE-CtP 16.151 μA (peak-to-peak separation of 0.454 V), GCE-CtP/Anti-IgG 11.915 μA (peak-to-peak separation of 0.566 V) and GCE-CtP/Anti-IgG/IgG 9.020 μA (peak-to-peak separation of 0.622 V). Cathodic current peaks were measured as follows; bare GCE 44.358 μA, GCE-CtP 20.006 μA, GCE-CtP/Anti-IgG 18.739 μA and GCE-CtP/Anti-IgG/IgG 14.154 μA. EIS data were also confirming these modifications as well as IgG recognition, as seen in Figure 4B. A drastic increase in Rct values in each step of the modification proves the successful covering, immobilization and selective interaction of the species. Rct values of Nyquist plots calculated for the designed biosensor were: Bare GCE: 380.1 Ω, GCE-CtP: 13290 Ω, GCE-CtP/Anti-IgG: 14620 Ω. Sensing ability to detect different concentrations of IgG was also investigated by immobilizing Anti-IgG antibody to polymer coated surface (GCE-CtP) and measuring the current change when different concentrations of IgG solutions were dropped on the GCE surface. As the concentration of the IgG solution increased, the difference in DPV signals between Anti-IgG coated and IgG bound GCE proportionally increased. Calibration curve given in Figure 5 was obtained using the current signal difference corresponding to the analyte concentration. The Linear range for the affinity-based sensor was found to be in between 0.05-2.50 ng/mL (linear plot was given as inset in Figure 5) and the equation for the linear fit was $y = 0.7822x + 0.2828$ with $R^2 = 0.986$. A drop in current responses was observed at higher IgG concentrations. This

could be due to the fact that analyte accumulation on the surface as a result of interactions between IgG molecules when higher amount of analyte was applied which prevents the diffusion of redox mediator to the electroactive surface.

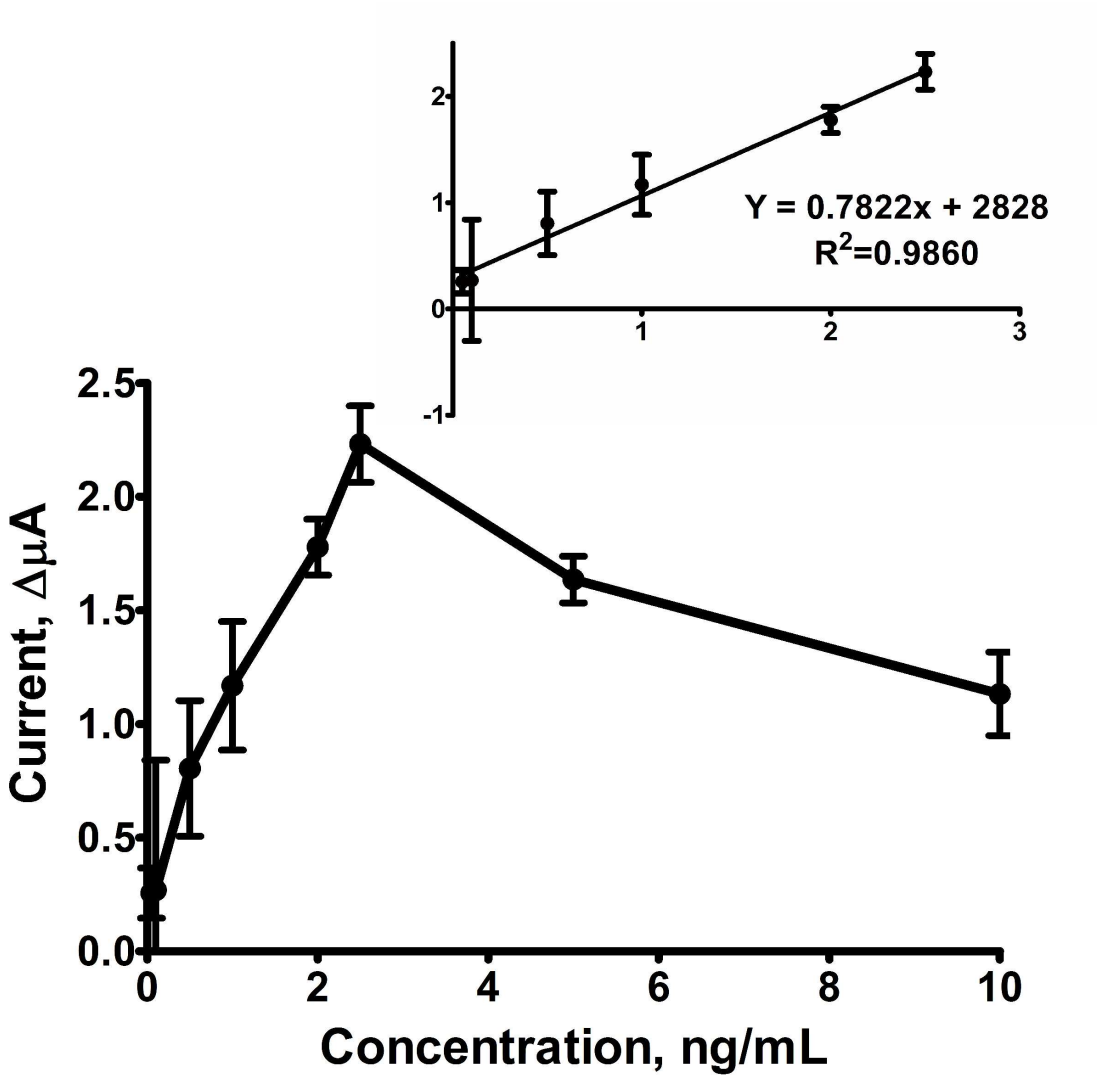

Figure 5. Calibration curve of GCE-CtP/Anti-IgG in response to different concentration of IgG solutions obtained by DPV measurements. Linear range was shown as inset (In 50 mM sodium phosphate buffer, pH 7.4, 25°C, Error bars show ± S.D).

Control experiments to test the selectivity of the proposed biosensor for both of the systems were conducted with possible interferants. Ascorbic acid (AA), uric acid (UA) and bovine serum albumin (BSA) were selected to be tested with the GOx activity-based sensing platform. They were added to the measurement probe of 10 mL of 50 mM sodium acetate buffer (pH 4.5) and enzymatic activity on the surface was monitored with the same principle, current signal response change, using the same experimental method with amperometric measurements. As shown in Figure 6A, there was no significant increase on the current signal from interfering compounds, compared to as of glucose at equal concentration. These results proved that, proposed enzymatic-activity based sensing platform selectively works with glucose more efficiently. With the same goal, selectivity test experiments were conducted with Anti-IgG modified GCE, using BSA and AA as interfering compounds. Using the same experimental procedure, these interferants were applied on the surface instead of IgG and current signal response changes were recorded. As seen in Figure 6B, no significant response was observed when interferants were applied on the surface compared to IgG at the same concentration, showing that this biosensor works selectively with Anti-IgG.

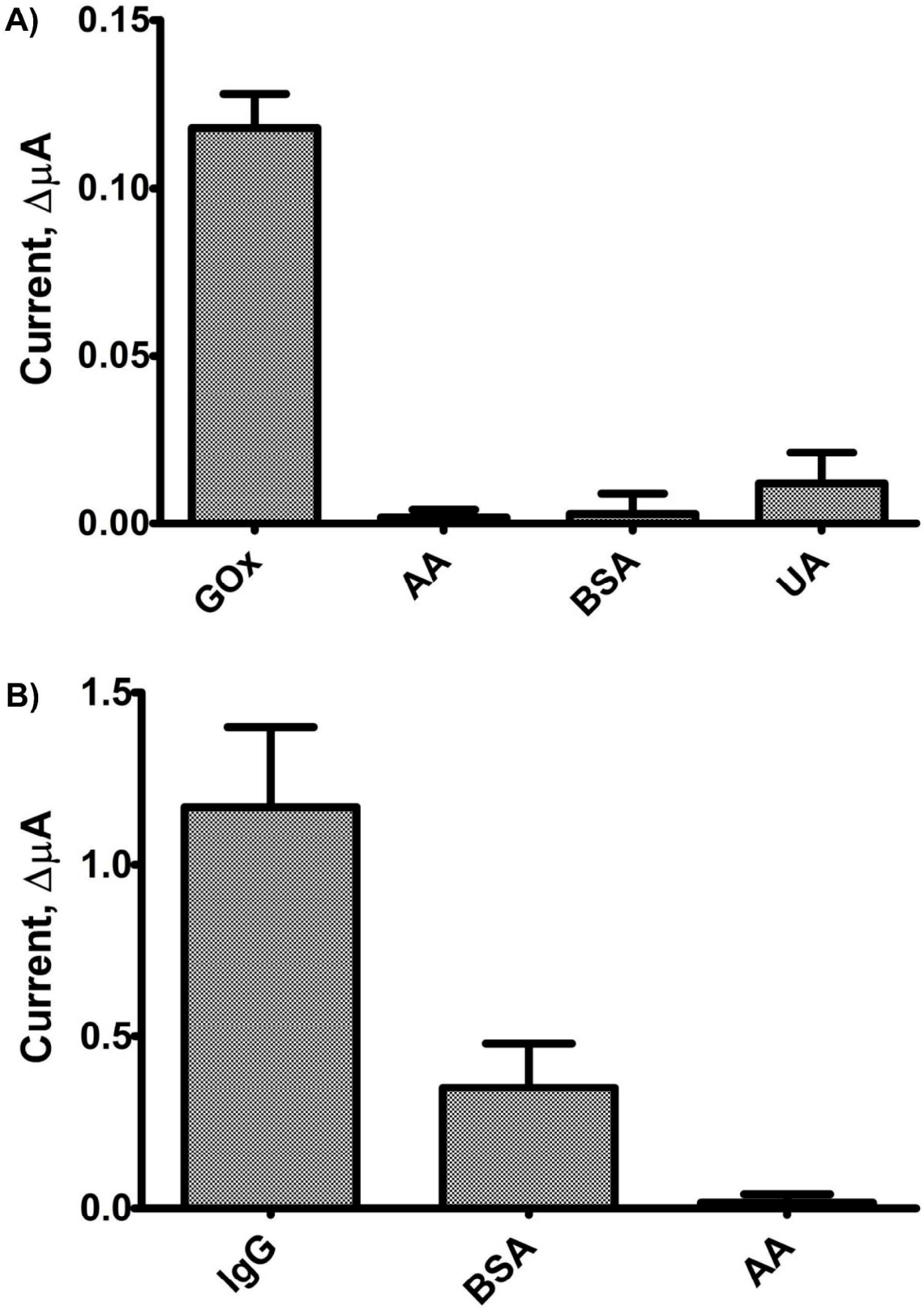
A)
0.15
0.10
0.05
0.00
Current, ΔμA
GOx
AA
BSA
UA
B)
1.5
1.0
0.5
0.0
Current, ΔμA
IgG
BSA
AA

Figure 6. A) Effect of interfering compounds on glucose biosensor; AA, BSA, and UA. The response signals were obtained via amperometric measurements. (In 50 mM sodium acetate buffer, pH 4.5, 25°C). B) Effect of interfering compounds on IgG biosensor; AA and BSA. The response signals were obtained via DPV. (In 50 mM sodium phosphate buffer, pH 7.4, 25°C) (Error bars show ± S.D.).

Contact angle measurements also provide substantial evidence for the changes of the surface characteristics that defined by the other techniques. As the synthesized polypeptide is highly hydrophilic, the contact angle is very low at the beginning. After immobilization of the biomolecules to the surface, contact angle increased due to their hydrophobic nature. As hydrophobic/hydrophilic amino acid ratio is different between the GOx and Anti-IgG, contact angles of two different biofunctional surfaces are different.

Table 1. Contact angle measurements of the surfaces with sessile drop method.

	Polymer coated GCE	*GOx bound*	*Anti-IgG bound*
CA Mean (^{o})	9.43	48.74	25.20
Std. Dev. (^{o})	1.27	4.46	5.58

XPS measurements. XPS measurements illustrate the crucial bonds used in conjugation steps. Elemental configuration analysis shows strong peaks at 284.08 eV, 399.08 eV and 532.08 eV indicating C1s, N1s and O1s binding energies. In Figure 6, C1s peaks of the surfaces are given. As shown in Figure 6A, CtP surface contained mostly sp^2 hybridized C-C bonds due to the

catechol group on the surface. Additionally, a considerable amount of sp^3 hybridized C-C bonds, C-N and C=N structures and C-O groups were found on the surface. GOx modified surface was analyzed in Figure 6B. GOx molecules were mostly occupied by sp^2 hybridized C-C, C-N and C=N groups. It also contains sp^2 hybridized C-C bonds and C-O groups. Finally, in Figure 6C, Anti-IgG antibody modified surface was explored. Unlike the first two, the majority of the surface was occupied by sp^3 hybridized C-C bonds due to the amino acid sequence. Furthermore, similar chemical groups were also observed, which are sp^2 hybridized C-C bonds, C-N and C-O groups. [53-56] The peak values were given in Table 2.

Table 2. C1S peaks of three different surfaces and functionalities.

CtP	CtP/GOx	CtP/Anti-IgG	Functionality
284.28 eV	284.38 eV	284.28 eV	C-C (SP^2)
285.28 eV	285.08 eV	284.88 eV	C-C (SP^3)
285.88 eV	285.98 eV	285.88 eV	C-N, C=N
287.28 eV	287.58 eV	287.58 eV	C-O
		286.38 eV	C-N, C=N

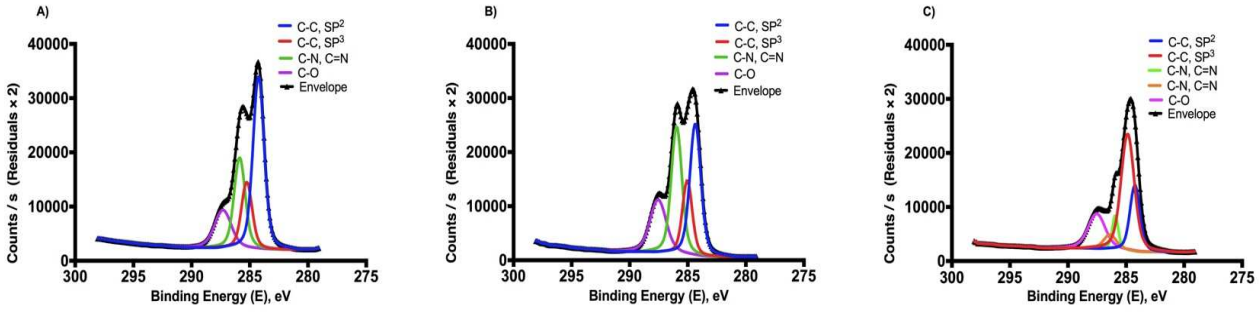

Figure 7. C1s peaks of the A) CtP, B) CtP-GOx, C) CtP-Anti-IgG structures using XPS. C=C (sp^2),

C-C (sp^3), C-N, C = N and C-O peaks were identified.

CONCLUSIONS

In conclusion, we described a novel methodology for the synthesis of a catechol-bearing polypeptide and created a unique functional surface for both enzyme activity- and affinity-based biosensor using GOx and Anti-IgG as model receptors, respectively. Both proposed systems worked properly and emerged as a promising selection for the sensors that will be developed in the future.

ASSOCIATED CONTENT

Supporting Information

The Supporting Information is available with the content of DPV curves and CV curves of varying scan rates.

AUTHOR INFORMATION

Corresponding Authors

* E-mail: suna.timur@ege.edu.tr and yusuf@itu.edu.tr

Author Contributions

All authors contributed equally.

ACKNOWLEDGMENT

Istanbul Technical University and Ege University Research Foundations are acknowledged for the financial support.

REFERENCES

(1) Dai, Y.; Xu, M.; Wei, J.; Zhang, H.; and Chen, Y. Surface modification of hydroxyapatite nanoparticles by poly(l-phenylalanine) via ROP of l-phenylalanine N-carboxyanhydride (Pha-NCA). *Appl. Surf. Sci*., **2012**, *258(7)*, 2850.

(2) Barbosa, M. E. M.; Montembault, V.; Cammas-Marion, S.; Ponchel, G.; and Fontaine, L. Synthesis and characterization of novel poly(γ-benzyl-L-glutamate) derivatives tailored for the preparation of nanoparticles of pharmaceutical interest. *Polym. Int*., **2007**, *56(3)*, 317.

(3) Ling, J.; Peng, H.; and Shen, Z. Deprotonation reaction of α-amino acid N-carboxyanhydride at 4-CH position by yttrium tris[bis(trimethylsilyl)amide]. *J. Polym. Sci., Part A: Polym. Chem.,* **2012**, *50*, 3743.

(4) Habraken, G. J. M.; Peeters, M.; Dietz, C. H. J. T.; Koning, C. E.; and Heise, A. How controlled and versatile is N-carboxy anhydride (NCA) polymerization at 0 °C? Effect of temperature on homo-, block- and graft (co)polymerization. *Polym. Chem*., **2010**, *1(4)*, 514.

(5) Obeid, R.; and Scholz, C. Synthesis and Self-Assembly of Well-Defined Poly(amino acid) End-Capped Poly(ethylene glycol) and Poly(2-methyl-2-oxazoline). *Biomacromolecules*, **2011**, *12(10)*, 3797.

(6) Vacogne, C. D.; Schlaad, H. Primary ammonium/tertiary amine-mediated controlled ring opening polymerisation of amino acid N-carboxyanhydrides. *Chemical Communications*, **2015**, *51(86)*, 15645-15648.

(7) Dimitrov, I.; Schlaad, H. Synthesis of nearly monodisperse polystyrene–polypeptide block copolymers via polymerisation of N-carboxyanhydrides. *Chemical Communications*, **2003**, *23*, 2944-2945.

(8) Ishikawa, K.; and Endo, T. Synthesis and polymerization of .gamma.-trichloroethyl-L-glutamate N-carboxyanhydride: a polypeptide that can be functionalized with a nucleophilic agent. *J. Am. Chem. Soc.*, **1988**, *110(6)*, 2016.

(9) Koga, K.; Sudo, A.; Nishida, H.; and Endo, T. Convenient and useful synthesis of N-carboxyanhydride monomers through selective cyclization of urethane derivatives of α-amino acids. *J. Polym. Sci., Part A: Polym. Chem*., **2009**, *47(15)*, 3839.

(10) Engels J. F.; Roose J.; Zhai D. S.; Yip K. M., Lee M. S.; Tang B. Z.; Renneberg R. Aggregation-induced emissive nanoparticles for fluorescence signaling in a low-cost paper-based immunoassay. *Colloids Surf., B*, **2016**, *143*, 440-446.

(11) Lin Z.; Lv S.; Zhang K. and Tang D. Optical transformation of a CdTe quantum dot-based paper sensor for a visual fluorescence immunoassay induced by dissolved silver ions. *J. Mater. Chem. B*, **2017**, *5*, 826.

(12) Zhang W.-H.; Ma W. and Long Y.-T. Redox-Mediated Indirect Fluorescence Immunoassay for the Detection of Disease Biomarkers Using Dopamine-Functionalized Quantum Dots. *Anal. Chem*. **2016**, *88*, 5131−5136.

(13) Yin Y.; Cao Y.; Xu Y. and Li G. Colorimetric Immunoassay for Detection of Tumor Markers. *Int. J. Mol. Sci,* **2010**, *11(12)*, 5077-5094.

(14) Liang J.; Wang Y. and Liu B. Paper-based fluoroimmunoassay for rapid and sensitive detection of antigen. *RSC Advances*, **2012**, *2*, 3878–3884.

(15) Liu J.; Mazumdar D.; Lu Y. A Simple and Sensitive "Dipstick" Test in Serum Based on Lateral Flow Separation of Aptamer-Linked Nanostructures. Angew. Chem., **2006**, *45(47)*, 7955-7959.

(16) Guler E.; Yilmaz Sengel T.; Gumus Z. P.; Arslan M.; Coskunol H., Timur S. and Yagci Y. Mobile Phone Sensing of Cocaine in a Lateral Flow Assay Combined with a Biomimetic Material. *Anal. Chem*. **2017**, *89*, 9629−9632.

(17) Srivastava M.; Nirala N. R.; SrivastavaS. K.; Prakash R. A Comparative Study of Aptasensor vs Immunosensor for Label-Free PSA Cancer Detection on GQDs-AuNRs Modified Screen-Printed Electrodes. *Sci. Rep.,* **2018**, *8*, 1923.

(18) Ding L.; Hao C.; Xue Y. and Ju H. A Bio-Inspired Support of Gold Nanoparticles-Chitosan Nanocomposites Gel for Immobilization and Electrochemical Study of K562 Leukemia Cells. *Biomacromolecules,* **2007**, *8*, 1341-1346.

(19) Wang, Q.-L.; Cui, H.-F.; Song, X.; Fan, S.-F.; Chen, L.-L.; Li, M.-M.; Li, Z.-Y. A label-free and lectin-based sandwich aptasensor for detection of carcinoembryonic antigen. *Sensors and Actuators B: Chemical*, **2018**, *260*, 48-54.

(20) Xia, N.; Deng, D.; Zhang, L.; Yuan, B.; Jing, M.; Du, J.; Liu, L. Sandwich-type electrochemical biosensor for glycoproteins detection based on dual-amplification of boronic acid-gold nanoparticles and dopamine-gold nanoparticles. *Biosensors and Bioelectronics*, **2013**, *43*, 155-159.

(21) Wei, W.; Dong, S.; Huang, G.; Xie, Q.; Huang, T. MOF-derived Fe2O3 nanoparticle embedded in porous carbon as electrode materials for two enzyme-based biosensors. *Sensors and Actuators B: Chemical*, **2018**, *260*, 189-197.

(22) Wei, Y.; Liu, X.-P.; Mao, C.; Niu, H.-L.; Song, J.-M.; Jin, B.-K. Highly sensitive electrochemical biosensor for streptavidin detection based on CdSe quantum dots. *Biosensors and Bioelectronics*, **2018**, *103*, 99-103.

(23) Qi, H.; Wang, C.; Cheng, N. Label-free electrochemical impedance spectroscopy biosensor for the determination of human immunoglobulin G. *Microchimica Acta*, **2010**, *170 (1-2),* 33-38.

(24) Kim, I.; Kwon, D.; Lee, D.; Lee, T. H.; Lee, J. H.; Lee, G.; Yoon, D. S. A highly permselective electrochemical glucose sensor using red blood cell membrane. *Biosensors and Bioelectronics*, **2018**, *102*, 617-623.

(25) Saei, A. A.; Dolatabadi, J. E. N.; Najafi-Marandi, P.; Abhari, Al.; de la Guardia M. Electrochemical biosensors for glucose based on metal nanoparticles. *TrAC Trends in Analytical Chemistry*, **2013**, *42*, 216-227.

(26) Dong, Y. P.; Huang, L.; Lei, Z. P.; Chu, X. F.; Zhang, Q. F. Electrochemical Biosensor of Glucose Based on the Immobilization of Glucose Oxidase on a Carbon Microsphere Modified Glassy Carbon Electrode. *Sensor Letters*, **2012**, *10(3-4)*, 1024-1030.

(27) Shan, C.; Yang, H.; Song, J.; Han, D.; Ivaska, A.; and Niu, L. Direct Electrochemistry of Glucose Oxidase and Biosensing for Glucose Based on Graphene. *Anal. Chem*., **2009**, *81(6),* 2378–2382.

(28) Liu, A.; Lang, Q.; Liang, B.; Shi, J. Sensitive detection of maltose and glucose based on dual enzyme-displayed bacteria electrochemical biosensor. *Biosensors and Bioelectronics*, **2017**, *87*, 25-30.

(29) Vidal, J. C.; Bonel, L.; Ezquerra, A.; Hernández, S.; Bertolín, J. R.; Cubel, C.; Castillo J. R. Electrochemical affinity biosensors for detection of mycotoxins: A review. *Biosensors and Bioelectronics*, **2013**, *49*, 146-158.

(30) Geng, P.; Zhang, X.; Teng, Y.; Fu, Y.; Xu, L.; Xu, M.; Jin, L.; Zhang, W. A DNA sequence-specific electrochemical biosensor based on alginic acid-coated cobalt magnetic beads for the detection of E. coli. *Biosensors and Bioelectronics*, **2011**, *26(7)*, 3325-3330.

(31) Wang, W.; Bao, T.; Zeng, X.; Xiong, H.; Wen, W.; Zhang, X.; Wang, S. Ultrasensitive electrochemical DNA biosensor based on functionalized gold clusters/graphene nanohybrids coupling with exonuclease III-aided cascade target recycling. *Biosensors and Bioelectronics,* **2017**, *91*, 183-189.

(32) Wanga, Z. W.; Zhang, J.; Guo, Y.; Wu, X. Y.; Yang, W. J.; Xu, L. J.; Chen, J. H.; Fu, F. F. A novel electrically magnetic-controllable electrochemical biosensor for the ultra sensitive and specific detection of attomolar level oral cancer-related microRNA. *Biosensors and Bioelectronics,* **2013**, *45*, 108-113.

(33) Huang, H.; Bai, W.; Dong, C.; Guo, R.; Liu, Z. An ultrasensitive electrochemical DNA biosensor based on graphene/Au nanorod/polythionine for human papillomavirus DNA detection. *Biosensors and Bioelectronics*, **2015**, *68*, 442-446.

(34) Liu, S.; Liu, J.; Han, X.; Cui, Y.; Wang, W. Electrochemical DNA biosensor fabrication with hollow gold nanospheres modified electrode and its enhancement in DNA immobilization and hybridization. *Biosensors and Bioelectronics*, **2010**, *25(7)*, 1640-1645.

(35) Ma W.; Ying Y.-L.; Qin L.-X.; Gu Z.; Zhou H.; Li D.-W.; Sutherland T. C.; Chen H.-Y. & Long Y.-T. Investigating electron-transfer processes using a biomimetic hybrid bilayer membrane system. *Nat. Protoc.,* **2013**, *8(3),* 439-450.

(36) Ma W.; Li D.-W.; Sutherland T. C.; Li Y.; Long Y.-T. and Chen H.-Y. Reversible Redox of NADH and NAD+ at a Hybrid Lipid Bilayer Membrane Using Ubiquinone. *J. Am. Chem. Soc.*, **2011**, *133*, 12366–12369.

(37) Luo W.; Zhu C.; Su S.; Li D.; He Y.; Huang Q. and Fan C. Self-Catalyzed, Self-Limiting Growth of Glucose Oxidase-Mimicking Gold Nanoparticles. *ACS Nano*, **2010**, *4(12),* 7451-7458.

(38) Maduraiveeran, G.; Sasidharan, M.; Ganesan, V. Electrochemical sensor and biosensor platforms based on advanced nanomaterials for biological and biomedical applications. *Biosensors and Bioelectronics,* **2018**, *103*, 113-129.

(39) Wang J. Electrochemical Glucose Biosensors. *Chem. Rev*., **2008**, *108*, 814−825.

(40) Zhang D.; Liu Q. Biosensors and bioelectronics on smartphone for portable biochemical detection. *Biosensors and Bioelectronics*, **2016**, *75*, 273-284.

(41) Putzbach, W.; and Ronkainen N. J. Immobilization Techniques in the Fabrication of Nanomaterial-Based Electrochemical Biosensors: A Review. *Sensors,* **2013**, *13(4),* 4811-4840.

(42) Drummond, T. G.; Hill, M. G.; and Barton, J. K. Electrochemical DNA sensors. *Nature Biotechnology,* **2003**, *21*, 1192–1199.

(43) Bozokalfa, G.; Akbulut, H.; Demir, B.; Guler, E.; Gumus, Z. P.; Odaci Demirkol, D.; Aldemir, E.; Yamada, S.; Endo, T.; Coskunol, H.; Timur, S.; and Yagci, Y. Polypeptide Functional Surface for the Aptamer Immobilization: Electrochemical Cocaine Biosensing. *Anal. Chem.*, **2016**, 88 (7), 4161–4167.

(44) Demir, B.; Yilmaz, T.; Guler, E.; Gumus, Z. P.; Akbulut, H.; Aldemir, E.; Coskunol, H.; Goen Colak, D.; Cianga, I.; Yamada, S.; Timur, S.; Endo, T.; Yagci, Y. Polypeptide with electroactive endgroups as sensing platform for the abused drug 'methamphetamine' by bioelectrochemical method. *Talanta,* **2016**, *161*, 789-796.

(45) Yilmaz, T.; Guler, E.; Gumus, Z. P.; Akbulut, H.; Aldemir, E.; Coskunol, H.; Goen Colak, D.; Cianga, I.; Yamada, S.; Timur, S.; Endo, T.; and Yagci, Y. Synthesis and application of a novel poly-L-phenylalanine electroactive macromonomer as matrix for the biosensing of 'Abused Drug' model. *Polym. Chem.*, **2016**, *7(47)*, 7304-7315.

(46) Guler, E.; Akbulut, H.; Bozokalfa, G.; Demir, B.; Oyman Eyrilmez, G.; Yavuz, M.; Odaci Demirkol, D.; Coskunol, H.; Endo, T.; Yamada, S.; Timur, S.; Yagci, Y. Bioapplications of Polythiophene-g-Polyphenylalanine-Covered Surfaces. *Macromol. Chem. Phys*. **2015***, 216*, 1868−1878.

(47) Chang, Q.; Nurumbetov G.; Simula A.; Zhu C.; Li M.; Wilson P.; Kempe K.; Yang B.; Tao L.; Haddleton D. M. Synthesis of well-defined catechol polymers forsurface functionalization of magnetic nanoparticles. *Polym. Chem*., **2016**, *7*, 7002.

(48) Xu C.; Xu K.; Gu H.; Zheng R.; Liu H.; Zhang X.; Guo Z. and Xu B. Dopamine as A Robust Anchor to Immobilize Functional Molecules on the Iron Oxide Shell of Magnetic Nanoparticles. *J. Am. Chem. Soc.*, **2004**, *126*, 9938–9939.

(49) Endres P. J.; Paunesku T.; Vogt S.; T. Meade J. and Woloschak G. E. DNA−TiO_2 Nanoconjugates Labeled with Magnetic Resonance Contrast Agents. *J. Am. Chem. Soc.*, **2007**, *129*, 15760–15761.

(50) Yamada, S.; Koga, K.; Endo, T. Useful synthetic method of polypeptides with well-defined structure by polymerization of activated urethane derivatives of α-amino acids. *J. Polym. Sci. Part A: Polym. Chem.* **2012**, *50*, 2527-2532.

(51) Yu, M.; Nowak, A. P.; Deming, T. J.; Pochan, D. J. Methylated Mono- and Diethyleneglycol Functionalized Polylysines: Nonionic, α-Helical, Water-Soluble Polypeptides. *J. Am. Chem. Soc.* **1999**, *121(51)*, 12210-12211.

(52) Akbulut H.; Yavuz M.; Guler E.; Odaci Demirkol D.; Endo T.; Yamada S.; Timur S. and Yagci Y. *Polym. Chem.*, **2014**, *5*, 3929.

(53) Christwardana, M.; Chung, Y.; and Kwon, Y. A new biocatalyst employing pyrenecarboxaldehyde as an anodic catalyst for enhancing the performance and stability of an enzymatic biofuel cell. *NPG Asia Materials,* **2017**, *9*, e386.

(54) Yilmaz, G.; Demir, B.; Timur, S.; Becer, C. R. Poly(methacrylic acid)-Coated Gold Nanoparticles: Functional Platforms for Theranostic Applications. *Biomacromolecules*, **2016**, *17 (9),* 2901–2911.

(55) Meng, L.; Xia, Y.; Liu, W.; Zhang, L.; Zou, P.; Zhang, Y. Hydrogen microexplosion synthesis of platinum nanoparticles/nitrogen doped graphene nanoscrolls as new amperometric glucose biosensor. *Electrochimica Acta*, **2015**, *152*, 330-337.

(56) Zhai, X.; Zhang, P.; Liu, C.; Bai, T.; Li, W.; Dai, L.; and Liu, W. Highly luminescent carbon nanodots by microwave-assisted pyrolysis. *Chem. Commun.*, **2012**, *48(64)*, 7955–7957.

TABLE OF CONTENTS